Supporting Information

Spectral and dynamical properties of multiexcitons in semiconductor nanorods

Krishan Kumar[1] and Maria Wächtler [2]**

[1]Department Functional Interfaces, Leibniz Institute of Photonic Technology Jena, Albert-Einstein-Straße 9, 07745 Jena, Germany

[2]Chemistry Department and State Research Center OPTIMAS, RPTU Kaiserslautern-Landau, Erwin-Schrödinger-Str. 52, 67663 Kaiserslautern

*Correspondence: kumar.krishan@leibniz-ipht.de, waechtler@phc.uni-kiel.de

Steady-state absorption and photoluminescence spectra

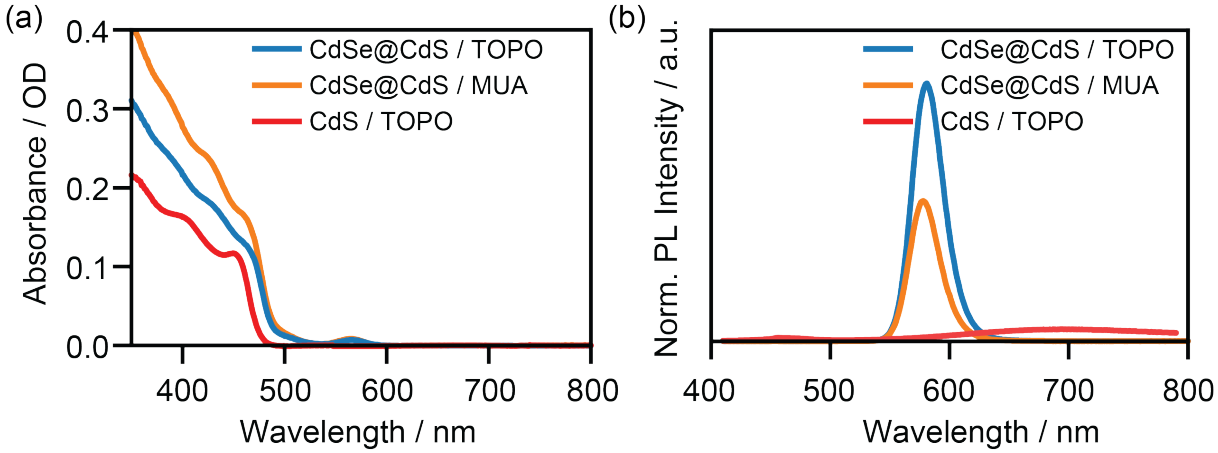

Figure S1. Optical properties of various nanorods. (a) Absorption spectra of TOPO-capped CdSe@CdS, MUA-capped CdSe@CdS nanorods, and TOPO-capped CdS nanorods. (b) Photoluminescence spectra of nanorods scaled by their respective absorbance at the excitation wavelength (400 nm).

TEM images

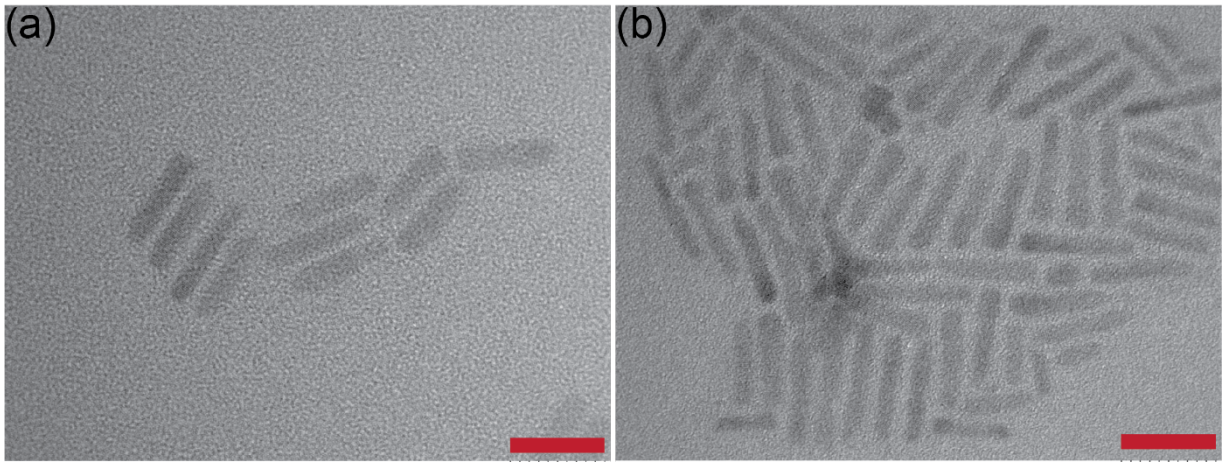

Figure S2. TEM images of (a) CdSe@CdS nanorods and (b) CdS nanorods used in the presented study. The scale bar shown in red is 20 nm.

IR spectra

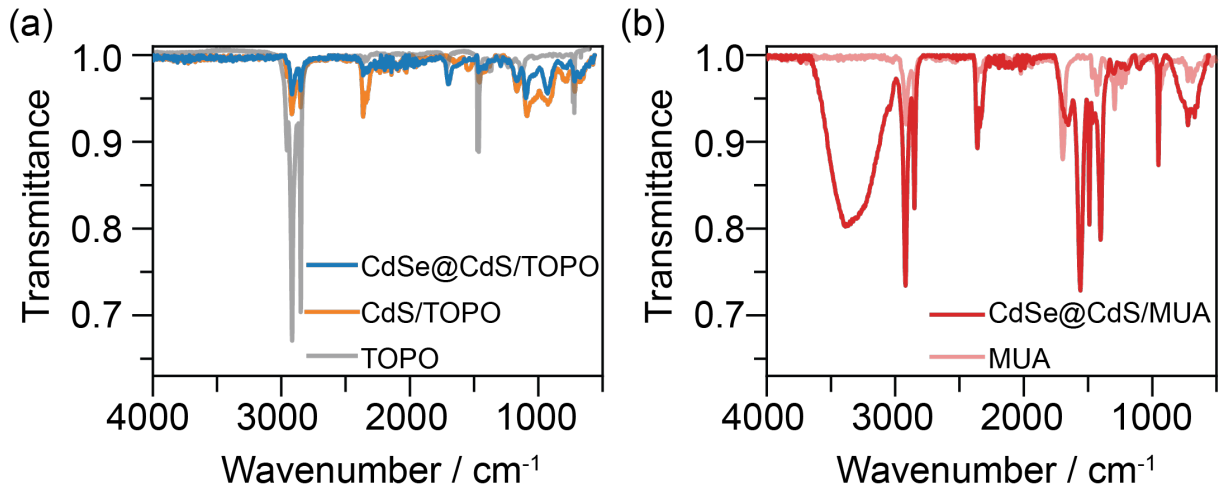

Figure S3. IR spectra of (a) CdSe@CdS nanorods and CdS nanorods functionalized with native surface ligands, and IR spectrum of pure TOPO, (b) CdSe@CdS nanorods after ligand exchange with MUA with MUA ligands and pure MUA ligands.

Comparisons of weight normalized TA spectra at 1000 ps following pump excitation:

The weight normalization is performed by multiplying with $1/(1-P_{N=0})$, calculated from the absorption cross-section resulting from the fit to normalize the transient spectra to the number of nanocrystals excited. At a delay of 1000 ps, the system has decayed to contain only monoexcitons, independent on the initial excitation of the individual nanocrystal, and signal intensity should here be proportional to the number of excited nanocrystals. Thus, normalized TA data should give identical spectra if the same species is present independent of the excitation intensity. However, the normalized TA signal of the CdSe@CdS nanorods show decreases in signal intensity with

increasing pump intensity (Figure S4), which shows that using only one long-lived component in a kinetic model most likely will not be able to describe the data satisfactorily.

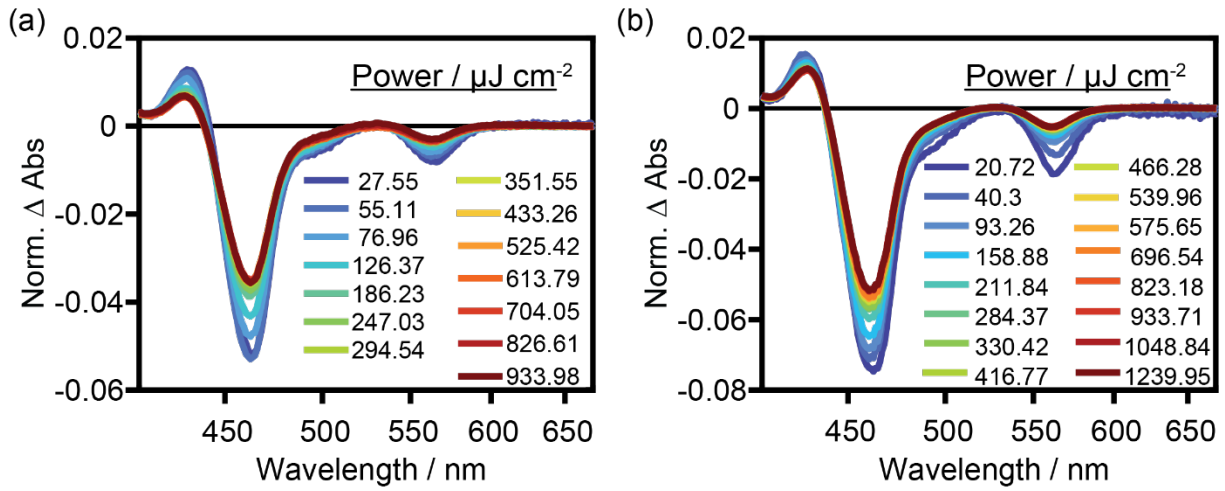

Figure S4. Transient absorption spectra at 1000 ps after excitation normalized to the total excited fraction for TOPO-capped (a) and MUA-capped (b) CdSe@CdS nanorods at different pump intensities. The normalization constant is $1/(1-P_{N=0})$, where $P_{N=0}$ is calculated using an optimized absorption cross-section.

Calculation of absorption cross-section

For MCMC sampling, the power density was used in µJ/cm^2 units, which was later converted to number of Photons/cm^2, to be able to use equation 2 described in the main text to calculate the absorption cross section units of 1/cm^2.

Power density in Photon/cm^2 is calculated as per the given formula:

$$P\left(\frac{photon}{cm^2}\right) = \frac{Laser\ power\ (\mu W) \times \lambda(nm) \times 10^{-7}}{h(Js) \times c(ms^{-1}) \times pump\ freq.(Hz) \times \pi \times \left({}^{d(\mu m)}/_{2}\right)^2}$$

Where h is Planck's constant, c is the speed of light, λ is the central pump wavelength, and d is the diameter of the Gaussian pump beam. The diameter of the pump beam was measured as 1/e^2

distance from the height intensity point using a beam profiler. The laser power was measured using a Gentec-EO (Canada) Maestro model connected to an XLP12-3S-VP-D0 thermal sensor.

Initial distribution of multi-excitonic species

The initial distribution of different exciton species can be calculated using the Poisson distribution based upon the average number of excitons <N> at that pump intensity. The following table (Table S1) shows the initial distribution of species sampled by the MCMC method for TOPO-capped CdSe@CdS nanorods.

Table S1. The average number of excitons <N> per nanorod and initial Poisson distribution of excitonic and multiexcitonic species for TOPO-capped CdSe@CdS nanorods, showing the increased contribution of higher-order multiexciton species with increasing pump intensity / average number of photons absorbed per nanorod.

Pump Intensity ($\mu J/cm^2$)	<N>	QX ($P_N \geq 4$)	TX ($P_N=3$)	BX ($P_N=2$)	X ($P_N=1$)	X_S
76.96	0.64	0.00	0.02	0.11	0.34	0
126.37	1.05	0.02	0.07	0.19	0.37	0
186.23	1.55	0.07	0.13	0.26	0.33	0
247.03	2.06	0.15	0.19	0.27	0.26	0
294.54	2.46	0.23	0.21	0.26	0.21	0
351.55	2.93	0.34	0.22	0.23	0.16	0
433.26	3.61	0.49	0.21	0.18	0.10	0
525.42	4.38	0.64	0.18	0.12	0.05	0
613.79	5.12	0.75	0.13	0.08	0.03	0
704.05	5.87	0.84	0.10	0.05	0.02	0
826.61	6.89	0.91	0.06	0.02	0.01	0
933.98	7.79	0.95	0.03	0.01	0.00	0

Kinetic fits and concentration profiles applying the model represented in scheme 1 of the main text:

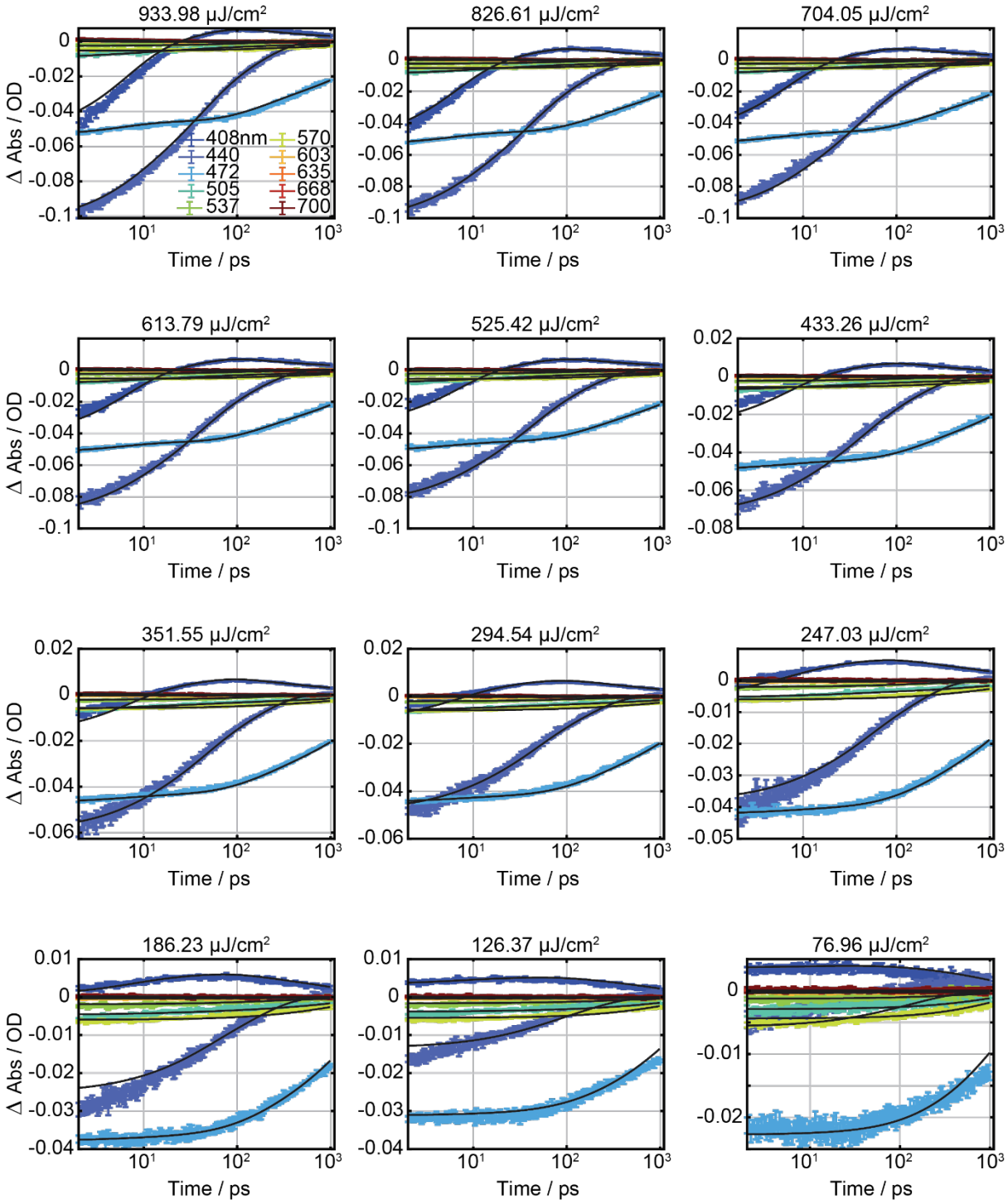

Figure S5. Kinetic traces and fits derived by Markov Chain Monte Carlo (MCMC) sampling of target model for TOPO-capped CdSe@CdS nanorods. Each panel shows the experimental data and black lines represent the kinetic fit traces. The fit lines are plotted by drawing 100 random samples from the Markov Chain overlaid on top of each other with the same colour and linewidth to visually show the deviations among randomly drawn samples.

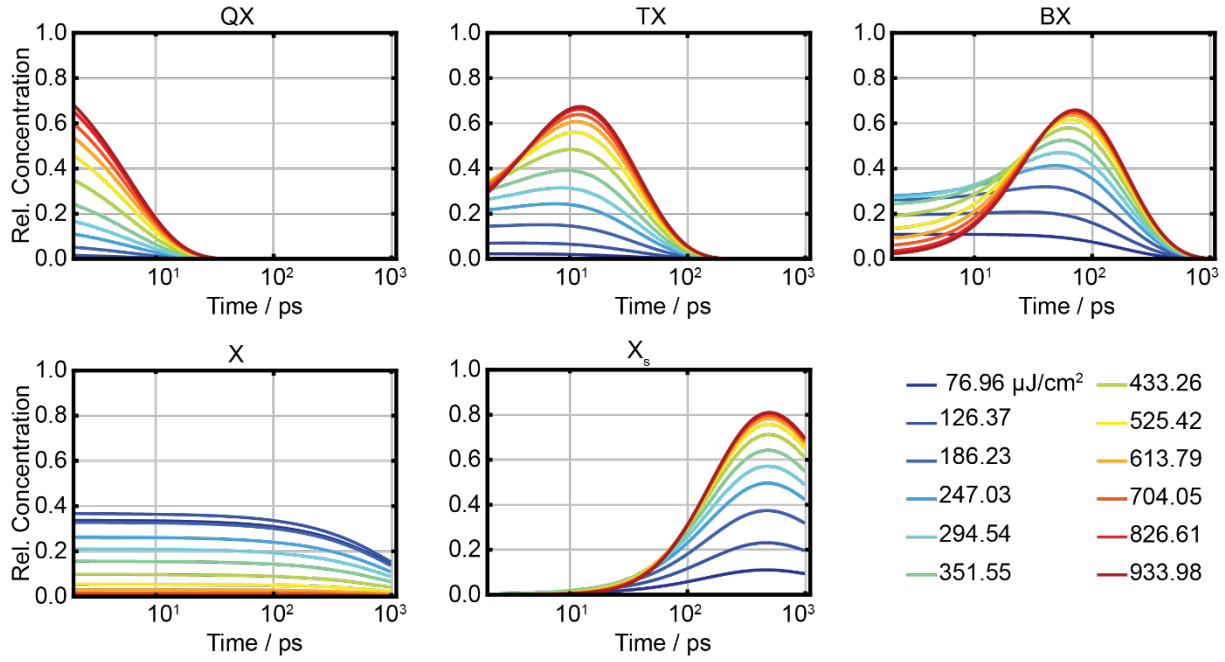

Figure S6. Intensity-dependent relative concentration profiles for TOPO-capped CdSe@CdS nanorods of various excitonic species. The concentration profiles drawn are generated by overlaying 100 random samples drawn from the Markov Chain.

Table S2. The average number of excitons <N> per nanorod and initial Poisson distribution of excitonic and multiexcitonic species for TOPO-capped CdS nanorods, showing the increased contribution of higher-order exciton species with increasing pump intensity or <N>.

Pump Intensity ($\mu J/cm^2$)	<N>	QX ($P_N \geq 4$)	TX ($P_N=3$)	BX ($P_N=2$)	X ($P_N=1$)	X_S
96.16	0.73	0.01	0.03	0.13	0.35	0
151.12	1.15	0.03	0.08	0.21	0.36	0
217.97	1.65	0.09	0.14	0.26	0.32	0
259.19	1.96	0.14	0.18	0.27	0.28	0
336.12	2.55	0.25	0.22	0.25	0.20	0
416.71	3.16	0.39	0.22	0.21	0.13	0
493.64	3.74	0.51	0.21	0.17	0.09	0
616.37	4.67	0.69	0.16	0.10	0.04	0
685.97	5.20	0.76	0.13	0.07	0.03	0
821.52	6.22	0.87	0.08	0.04	0.01	0
892.04	6.76	0.90	0.06	0.03	0.01	0
1062.39	8.05	0.96	0.03	0.01	0.00	0

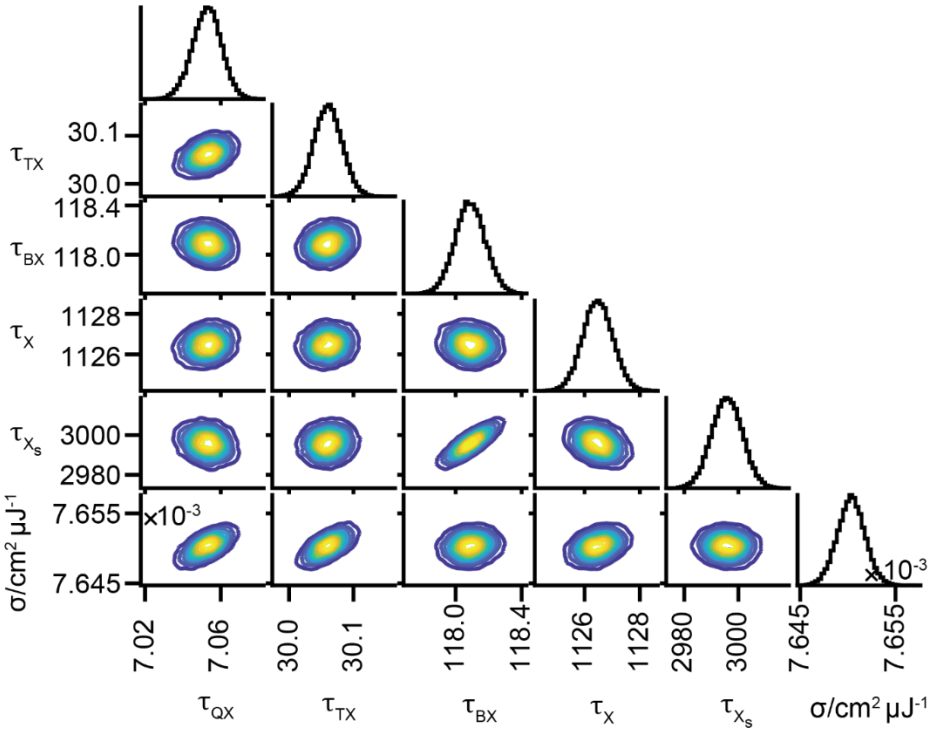

Figure S7. Corner plot of the posterior probability distribution of modelled parameters 96 – 1060 $\mu J/cm^2$ obtained from MCMC sampling of the target model for TOPO-capped CdS nanorods.

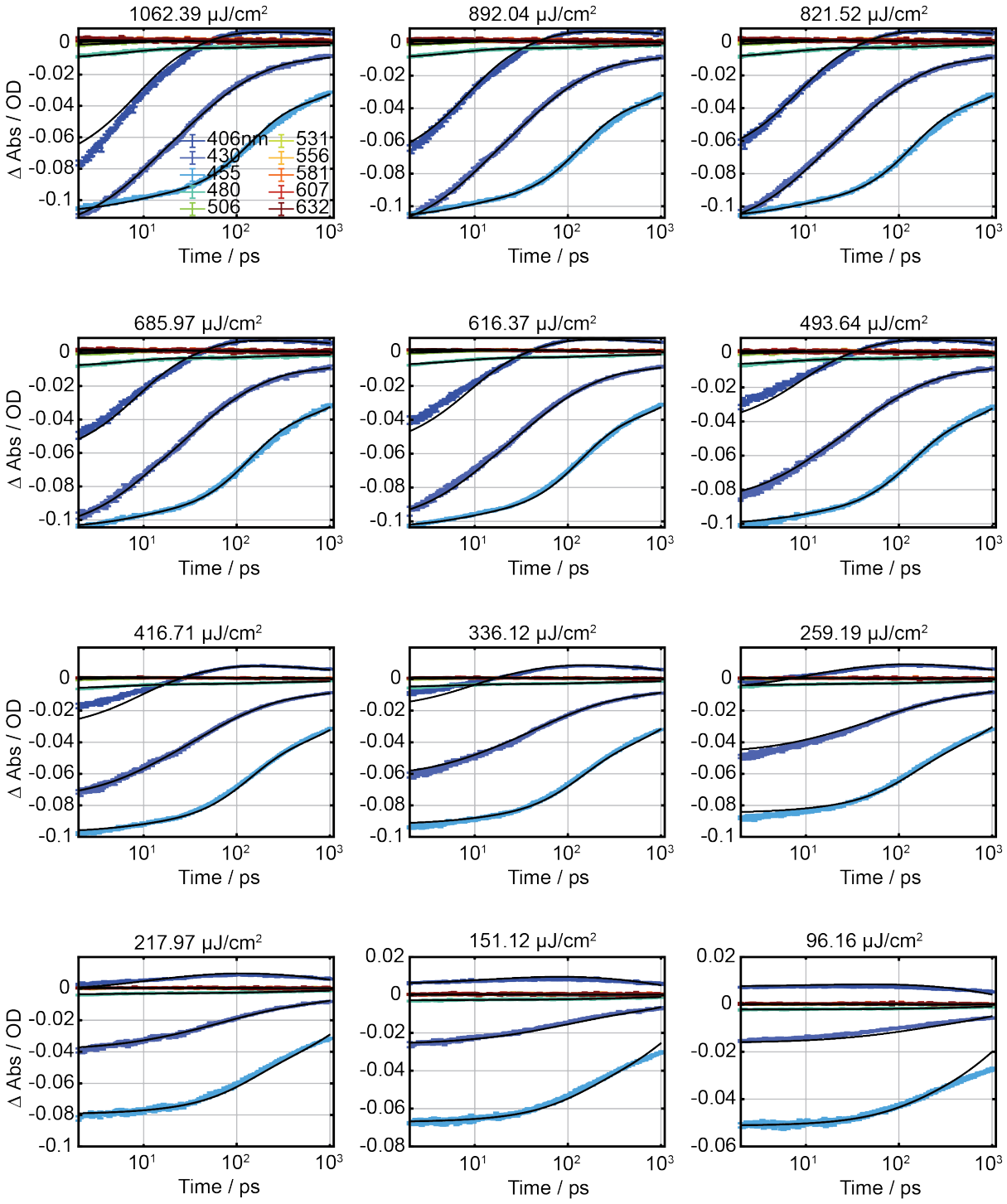

Figure S8. Kinetic traces and fits derived by Markov Chain Monte Carlo (MCMC) sampling of target model for TOPO-capped CdS nanorods. Each panel shows the experimental data and black lines represent the kinetic fit traces. The fit lines are plotted by drawing 100 random samples from the Markov Chain overlaid on top of each other with the same colour and linewidth to visually show the deviations among randomly drawn samples.

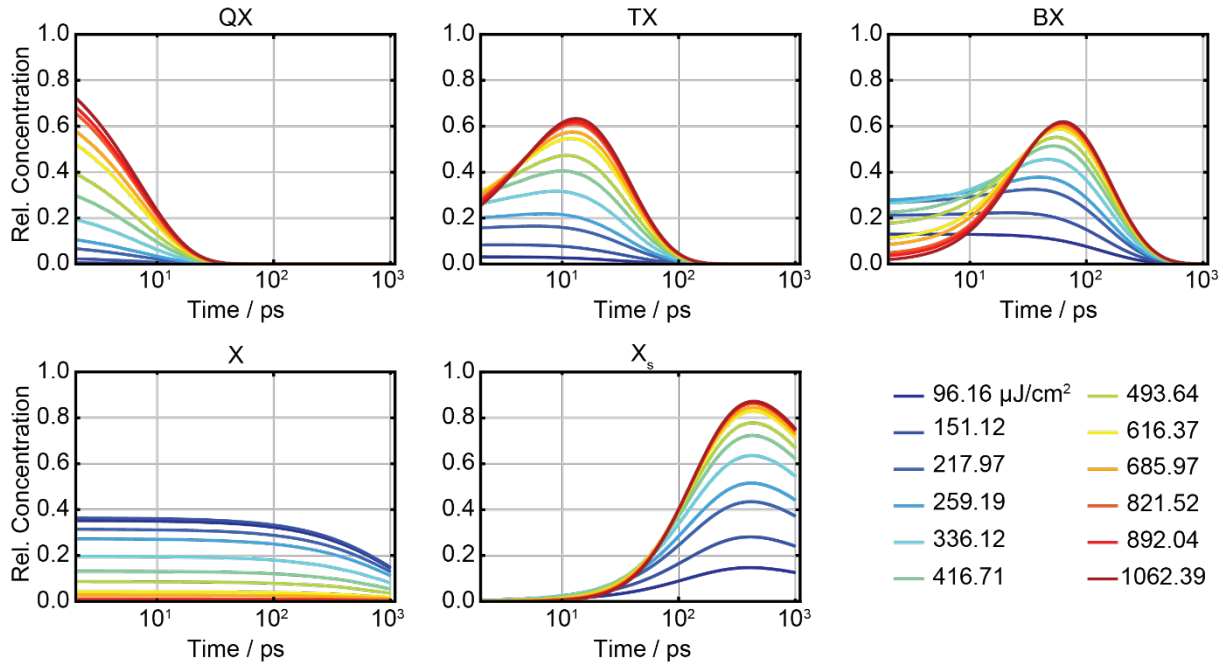

Figure S9. Intensity-dependent relative concentration profiles for TOPO-capped CdS nanorods of various excitonic species. The concentration profiles drawn are generated by overlaying 100 random samples drawn from the Markov Chain.

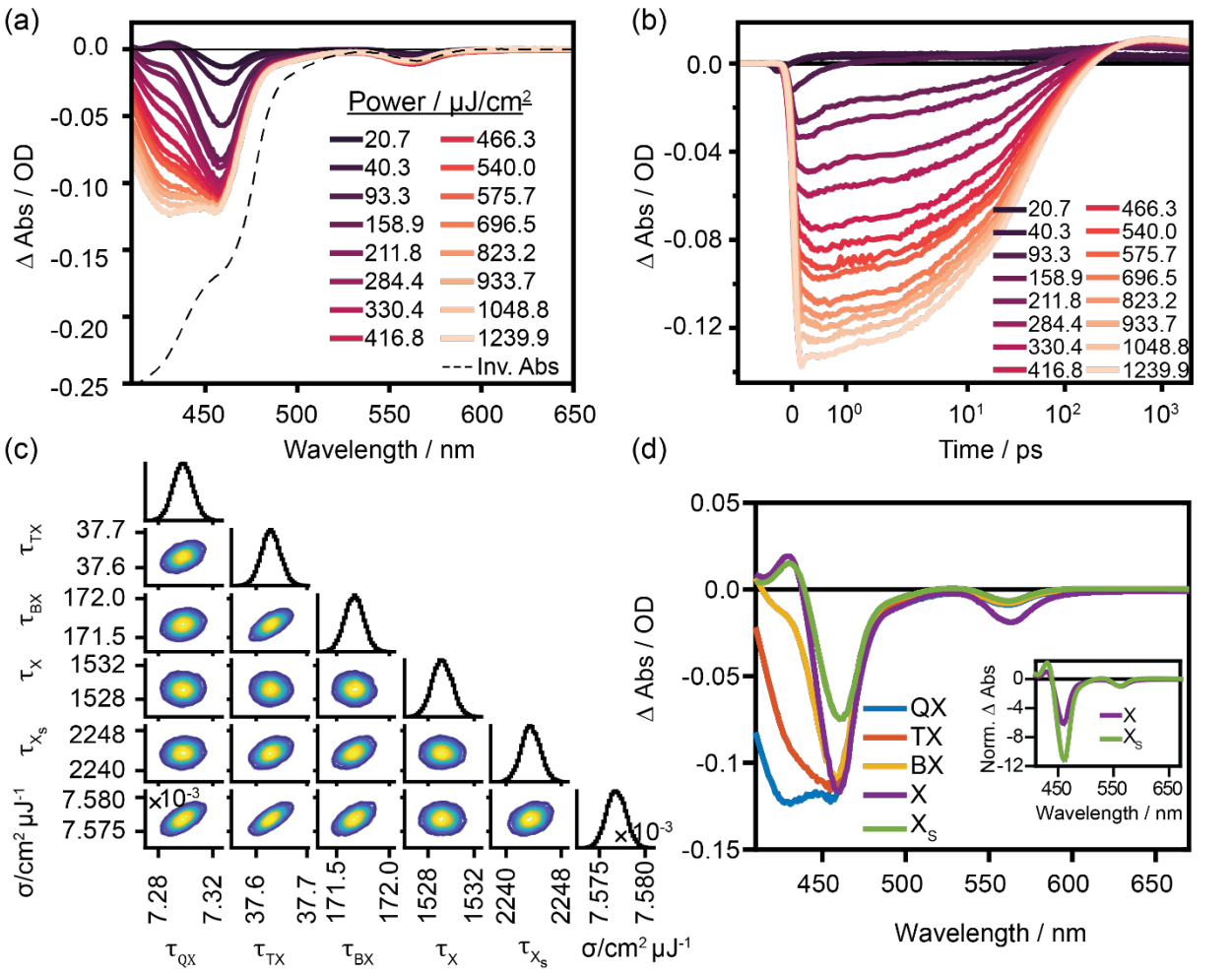

Figure S10. Intensity-dependent transient absorption data for MUA capped CdSe@CdS nanorods dispersed in methanol excited with 400 nm pump pulse. (a) TA spectra 2 ps after excitation, (b) kinetic decay of the photoinduced absorption band at 432 nm with increasing pump intensity, (c) corner plot of the posterior probability distribution of modelled parameters 93 – 1240 μJ/cm2 from MCMC sampling of the target model and (d) component spectra of modelled species. Inset: component spectra of X and X_S at CdSe band normalized at edge bleach. The tetra-exciton (blue trace), tri-exciton (red trace), bi-exciton (orange trace), mono-exciton X (purple trace), and surface mono-exciton (green trace) all are plotted by drawing 100 random samples from the Markov Chain and overlaid on top of each other with same colour and linewidth, to visually show the deviations among randomly drawn samples.

Table S3. The average number of excitons <N> per nanorod and initial Poisson distribution of excitonic and multiexcitonic species for MUA capped CdSe@CdS nanorods, showing the increased contribution of higher-order exciton species with increasing pump intensity or <N>.

CdSe@CdS/MUA						
Pump Intensity ($\mu J/cm^2$)	<N>	QX ($P_N \geq 4$)	TX ($P_N=3$)	BX ($P_N=2$)	X ($P_N=1$)	X_S
93.17	0.71	0.01	0.03	0.12	0.35	0
158.77	1.21	0.03	0.09	0.22	0.36	0
211.53	1.62	0.08	0.14	0.26	0.32	0
284.04	2.17	0.17	0.19	0.27	0.25	0
330.66	2.53	0.25	0.22	0.25	0.20	0
416.88	3.19	0.40	0.22	0.21	0.13	0
466.44	3.57	0.48	0.21	0.18	0.10	0
539.72	4.13	0.59	0.19	0.14	0.07	0
575.26	4.40	0.64	0.17	0.12	0.05	0
695.76	5.32	0.78	0.12	0.07	0.03	0
823.57	6.30	0.87	0.08	0.04	0.01	0
933.90	7.14	0.93	0.05	0.02	0.01	0
1048.81	8.02	0.96	0.03	0.01	0.00	0
1240.40	9.49	0.99	0.01	0.00	0.00	0

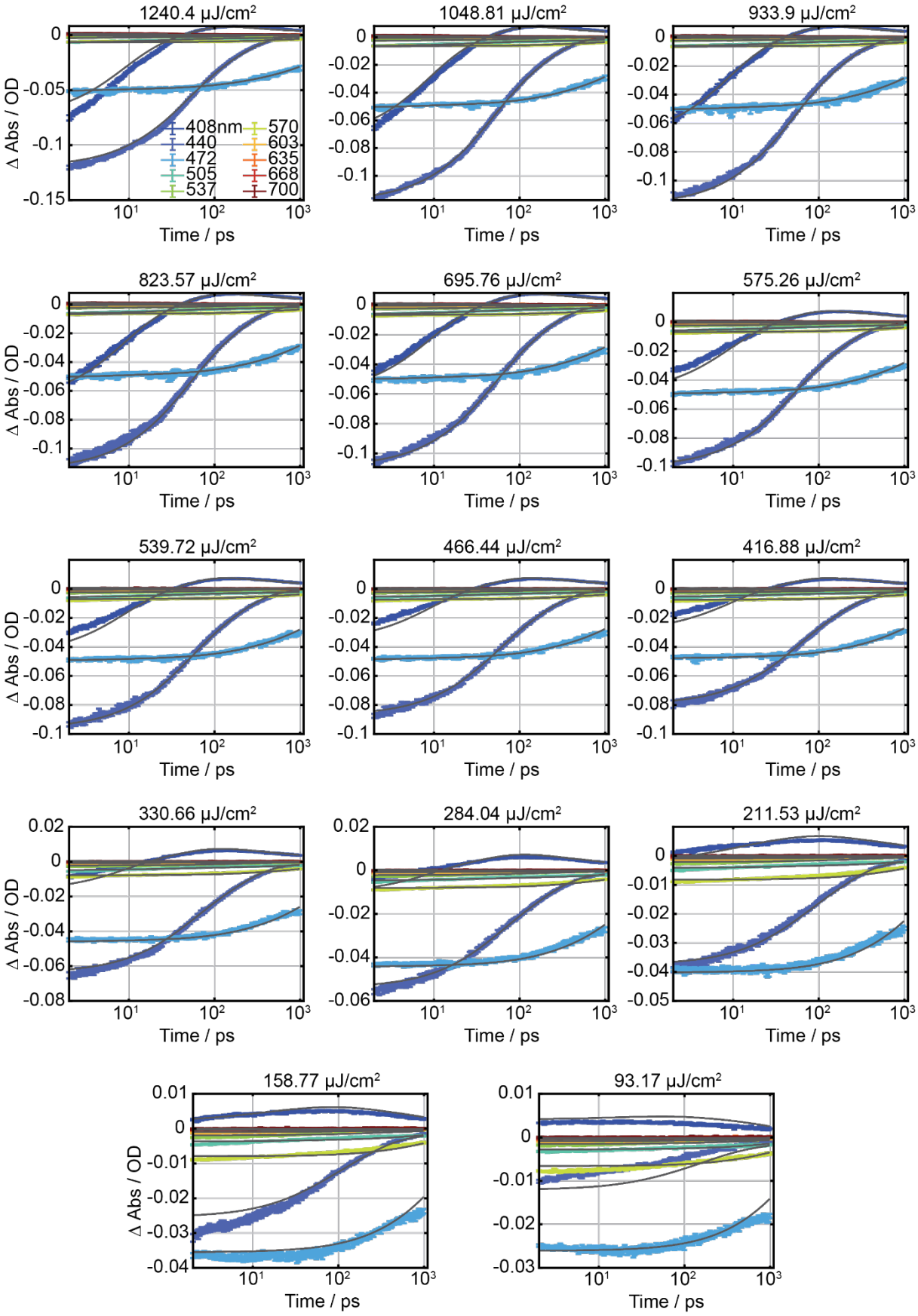
1240.4 µJ/cm²
1048.81 µJ/cm²
933.9 µJ/cm²
823.57 µJ/cm²
695.76 µJ/cm²
575.26 µJ/cm²
539.72 µJ/cm²
466.44 µJ/cm²
416.88 µJ/cm²
330.66 µJ/cm²
284.04 µJ/cm²
211.53 µJ/cm²
158.77 µJ/cm²
93.17 µJ/cm²
Δ Abs / OD
Time / ps
408nm
440
472
505
537
570
603
635
668
700

Figure S11. Kinetic traces and fits derived by Markov Chain Monte Carlo (MCMC) sampling of target model for MUA-capped CdSe@CdS nanorods. Each panel shows the experimental data and black lines represent the kinetic fit traces. The fit lines are plotted by drawing 100 random samples from the Markov Chain overlaid on top of each other with the same colour and linewidth to visually show the deviations among randomly drawn samples.

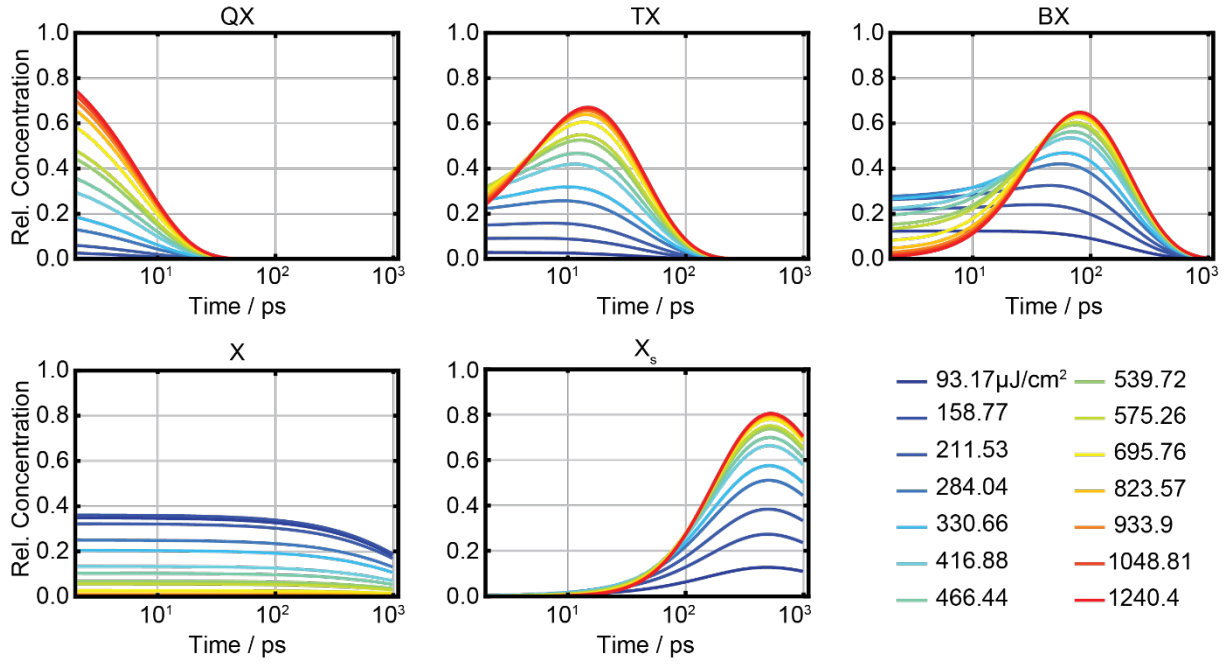

Figure S12. Intensity-dependent relative concentration profiles for MUA-capped CdSe@CdS nanorods of various excitonic species. The concentration profiles drawn are generated by overlaying 100 random samples drawn from the Markov Chain.

Sample stability and illumination-induced effects

To explore the presence of irradiation-induced effects, pump-intensity dependent datasets for pre-illuminated samples and non-illuminated samples, both TOPO-capped CdSe@CdS and CdS nanorods, are compared. The absorption spectra show only slight changes in the UV region (Figure S13). The general electronic structure of the nanorods remains intact upon illumination. The absorption spectrum shows that the characteristic absorption features of nanorods are preserved.

The absorption spectra of CdSe@CdS nanorods show a slightly enhanced absorption band, and CdS nanorods show a slight (3 nm) blue shift of the first excitonic peak.

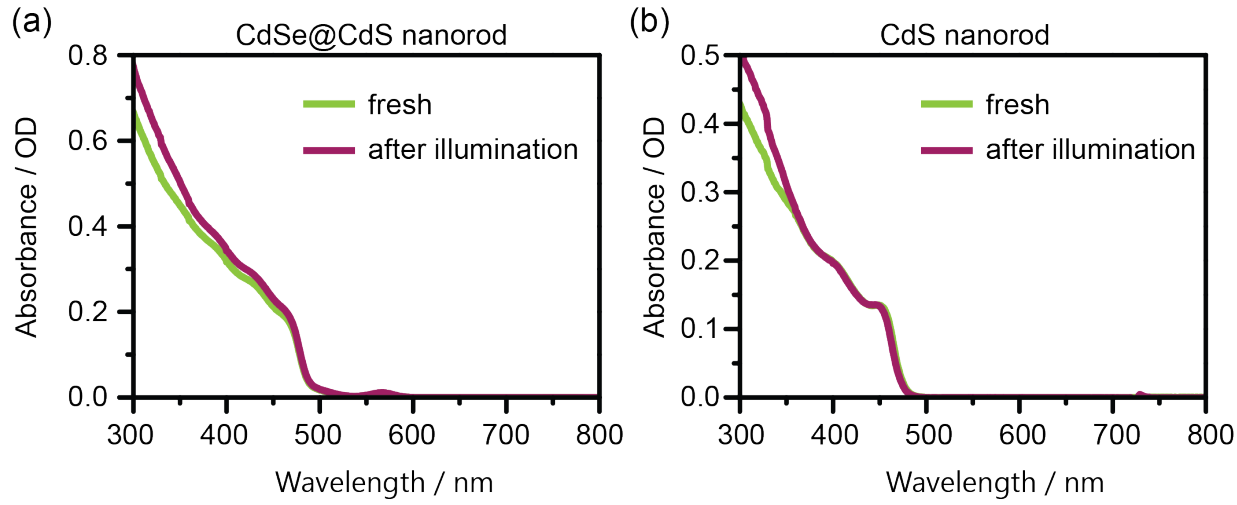

Figure S13. Absorption spectra before and after illumination with intense pump pulse at 400 nm (750 μJ/cm^2) for 3 hours and left the sample in inert conditions overnight to observe the non-reversible effects of laser illumination on the sample for (a) TOPO-capped CdSe@CdS nanorods, (b) TOPO-capped CdS nanorods.

In the transient absorption experiment, quantitatively similar behavior with increasing pump pulse intensity compared to non-illuminated samples is observed (see Figure S14). The same kinetic model as in Scheme 1 in the main text, just with a decreased number multiexciton orders regarded due to the limitation of this experiment to a lower excitation intensity region (15–270 μJ/cm^2), is used to model the intensity-dependent TA data. The kinetic fits, the relative concentration profiles, and the lifetime of the modelled species are presented in Table S4, Figure S15–S22. The comparison of species-associated spectra normalized to their respective triexciton bleach before and after the illumination is presented in Figure S23. No significant differences, neither in the time components nor in the spectral components, can be found. Only in the transient species spectra are

slight differences in the intensity of the CdS bleach component visible, which most likely are within the limits of the experimental fluctuations within different data sets.

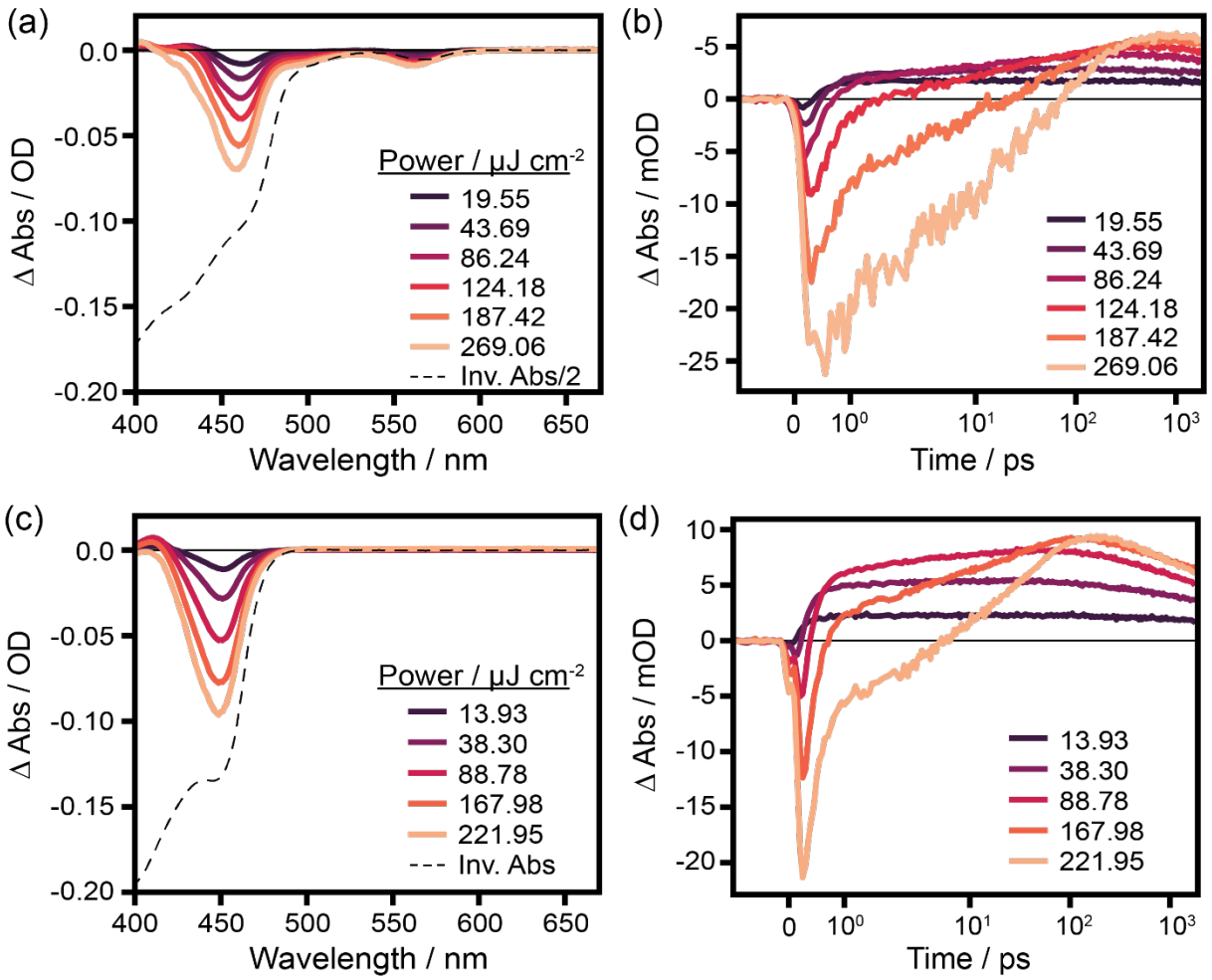

Figure S14. Intensity-dependent transient absorption data of pre-illuminated TOPO capped CdSe@CdS (a, b) and CdS (c, d) nanorods dispersed in toluene excited with 400 nm pump pulses. (a) TA spectra of CdSe@CdS nanorods after 2 ps excitation, (b) kinetic decay of 432 nm with increasing pump intensity, (c) TA spectra of CdS nanorods after 2 ps excitation and (d) kinetics of photoinduced absorption band at 413 nm.

Table S4. Fitted median values and 95% confidence interval of modelled parameters extracted from MCMC Sampling of 3 h pre-illuminated TOPO-capped CdSe@CdS and CdS nanorods.

Parameter Name	CdSe@CdS NR		CdS NR	
	Non-illuminated	Illuminated	Non-illuminated	Illuminated
$\tau_{triexciton}/ps$[a]	$25.79^{25.94}_{25.65}$	$15.43^{15.48}_{15.38}$	$27.85^{27.96}_{27.74}$	$30.06^{30.17}_{29.95}$
$\tau_{biexciton}/ps$	$182.6^{183.6}_{181.6}$	$183.4^{183.9}_{182.9}$	$145.0^{145.5}_{144.5}$	$184.4^{185.2}_{183.7}$
$\tau_{monoexciton}/ps$[b]	1545^{1551}_{1540}	1122^{1124}_{1119}	2133^{2139}_{2127}	2455^{2463}_{2448}
$\tau_{surface\ exciton}/ps$[b]	3449^{3493}_{3407}	3619^{3646}_{3593}	4939^{5055}_{4830}	11122^{11669}_{10629}
Absorption cross-section (σ)/cm^{2}μJ^{-1}	$10.78 \times 10^{-3}\ ^{10.80\times 10^{-3}}_{10.76\times 10^{-3}}$	$8.21 \times 10^{-3}\ ^{8.23\times 10^{-3}}_{8.20\times 10^{-3}}$	$7.04 \times 10^{-3}\ ^{7.06\times 10^{-3}}_{7.02\times 10^{-3}}$	$9.80 \times 10^{-3}\ ^{9.82\times 10^{-3}}_{9.78\times 10^{-3}}$

a) represents included contribution of higher order excitons which are not explicitly modelled, b) represents out of modelled time window values.

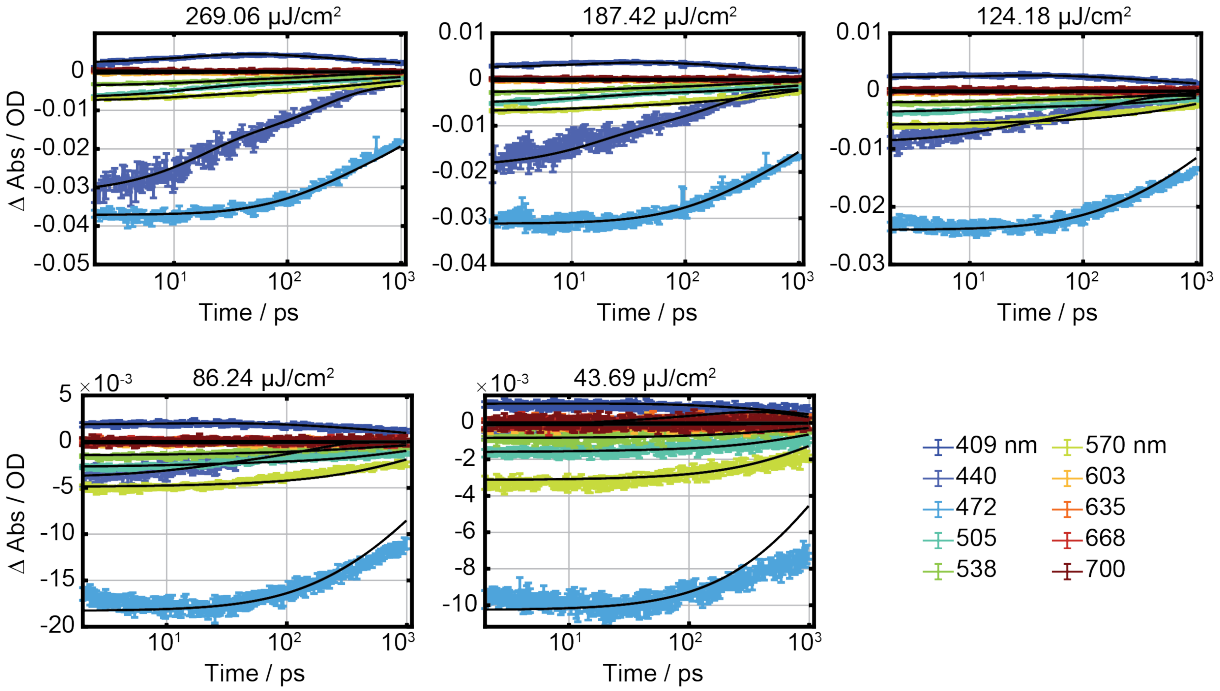

Figure S15. Kinetic traces and fits derived by Markov Chain Monte Carlo (MCMC) sampling of target model for pre-illuminated TOPO-capped CdSe@CdS nanorods. Each panel shows the experimental data and black lines represent the kinetic fit traces. The fit lines are plotted by drawing 100 random samples from the Markov Chain overlaid on top of each other with the same colour and linewidth to visually show the deviations among randomly drawn samples.

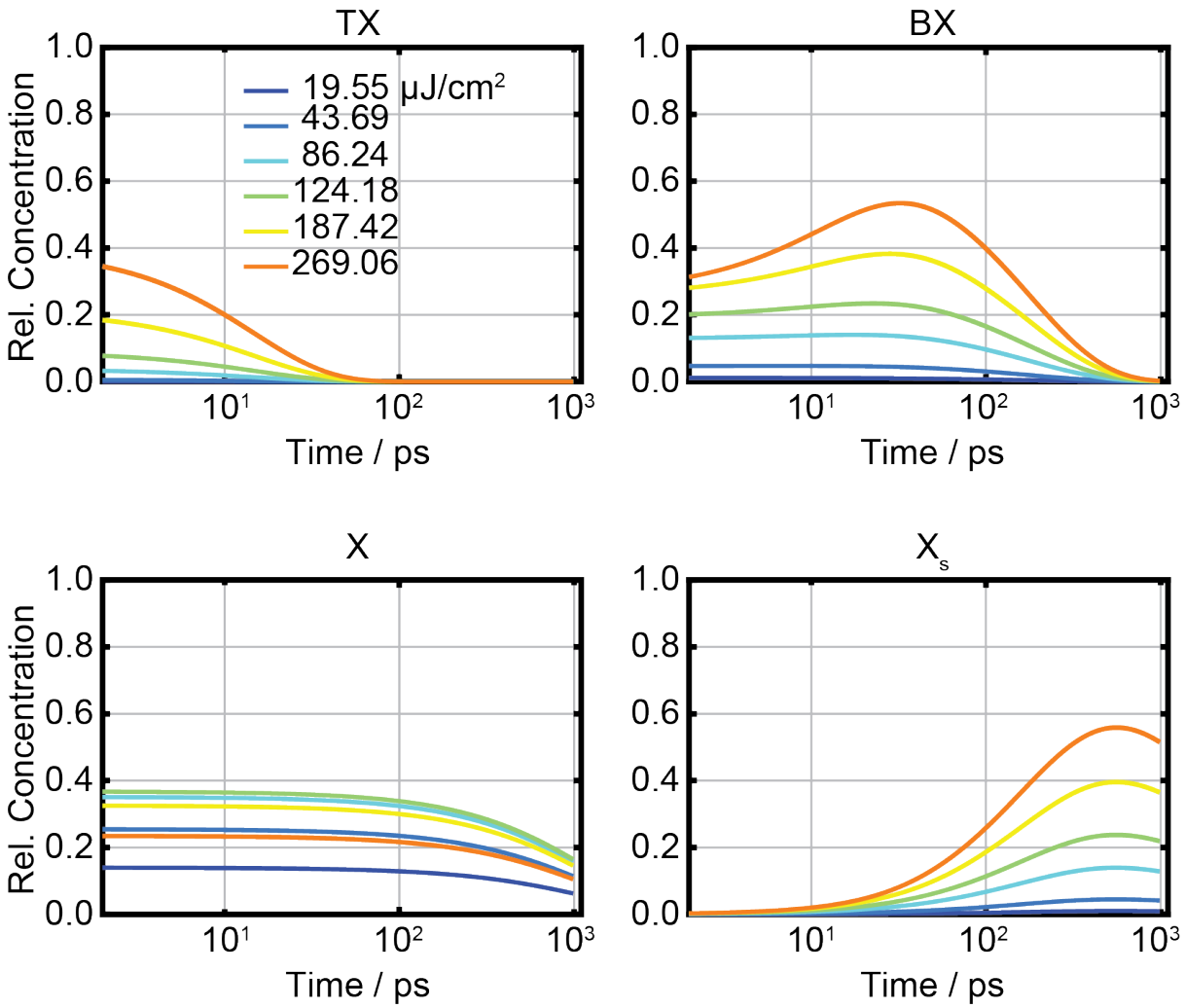

Figure S16. Intensity-dependent concentration profiles for pre-illuminated TOPO-capped CdSe@CdS nanorods for various excitonic species. The concentration profiles are overlaid from 100 random samples drawn from the Markov Chain.

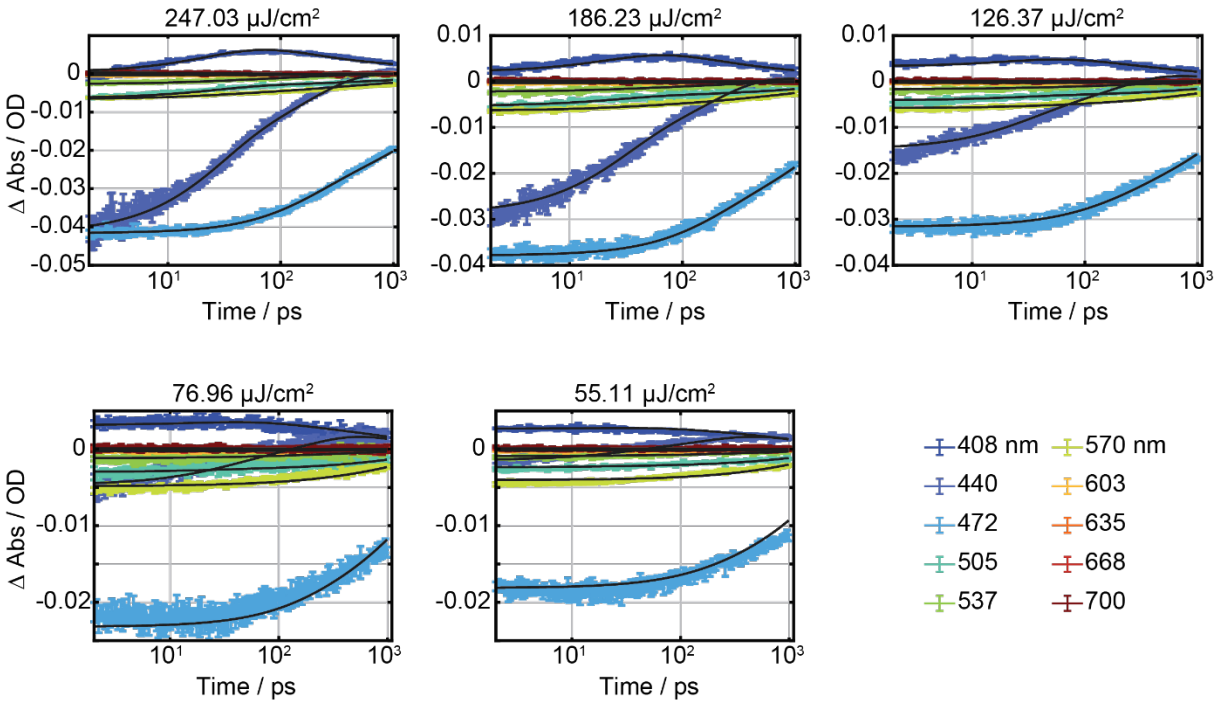

Figure S17. Kinetic traces and fits derived by Markov Chain Monte Carlo (MCMC) sampling of target model for non-illuminated TOPO-capped CdSe@CdS nanorods. Each panel shows the experimental data and black lines represent the kinetic fit traces. The fit lines are plotted by drawing 100 random samples from the Markov Chain overlaid on top of each other with the same colour and linewidth to visually show the deviations among randomly drawn samples.

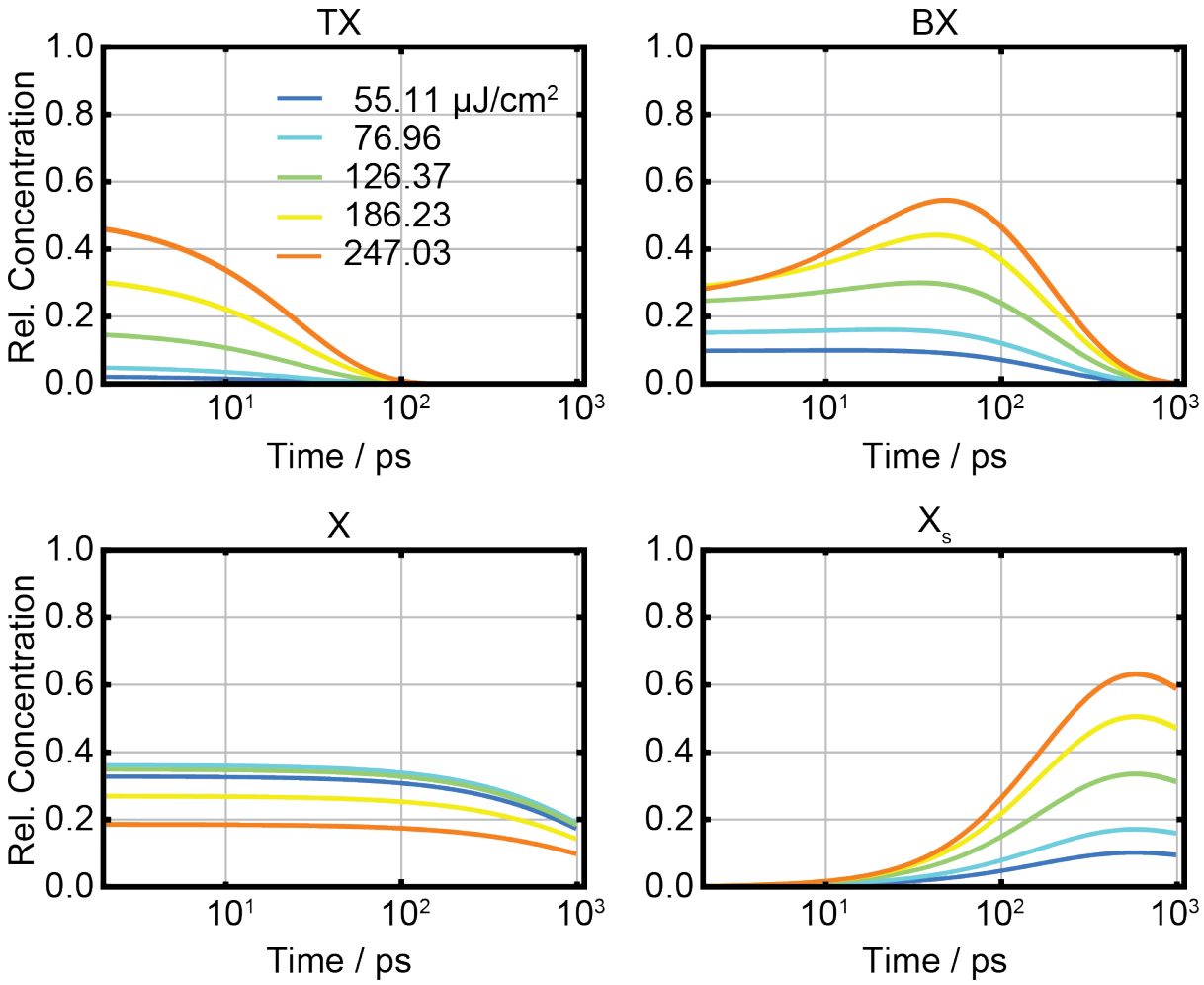

Figure S18. Intensity-dependent concentration profiles for non-illuminated TOPO-capped CdSe@CdS nanorods are used to make a direct comparison to the pre-illuminated sample. Excitonic species are given at the top of each panel. The concentration profiles are overlaid from 100 random samples drawn from the Markov Chain.

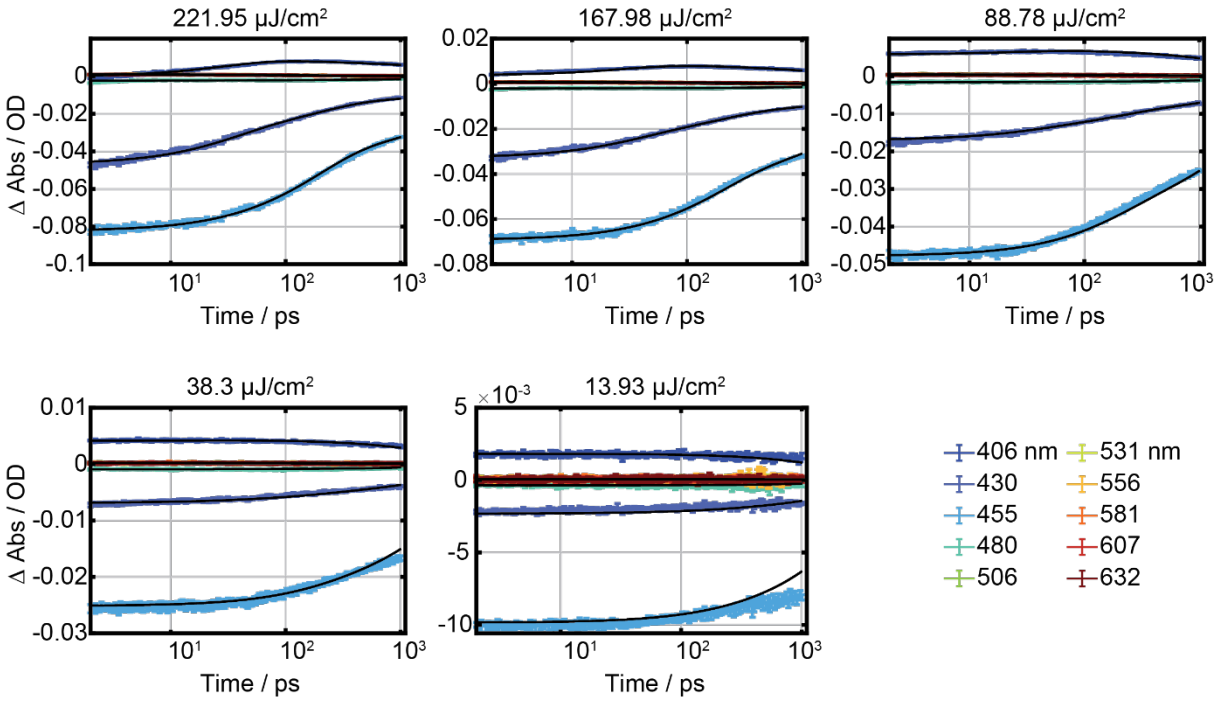

Figure S19. Kinetic traces and fits derived by Markov Chain Monte Carlo (MCMC) sampling of target model for pre-illuminated TOPO-capped CdS nanorods. Each panel shows the experimental data and black lines represent the kinetic fit traces. The fit lines are plotted by drawing 100 random samples from the Markov Chain overlaid on top of each other with the same colour and linewidth to visually show the deviations among randomly drawn samples.

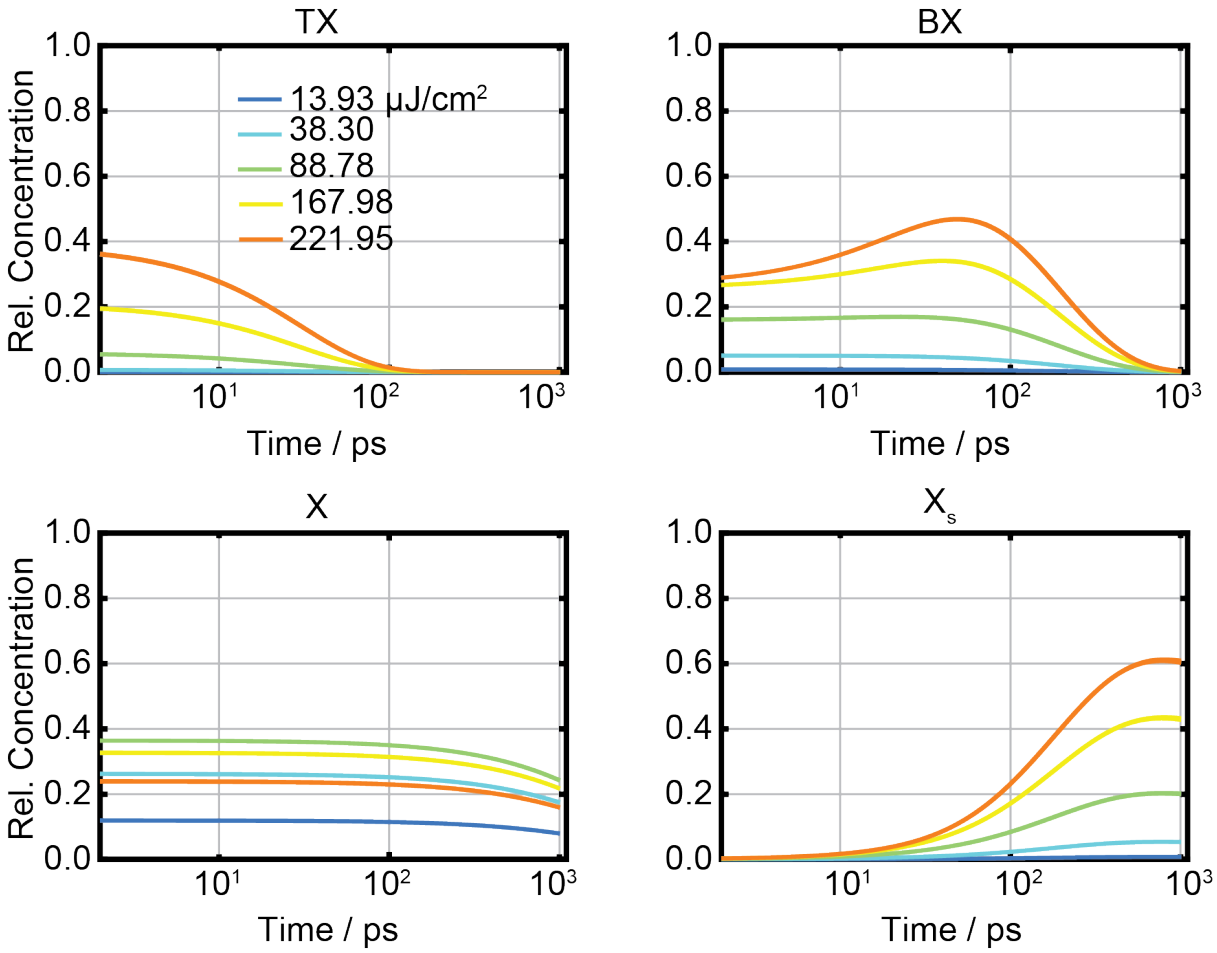

Figure S20. Intensity-dependent concentration profiles for pre-illuminated TOPO-capped CdS nanorods for various excitonic species. The concentration profiles are overlaid from 100 random samples drawn from the Markov Chain.

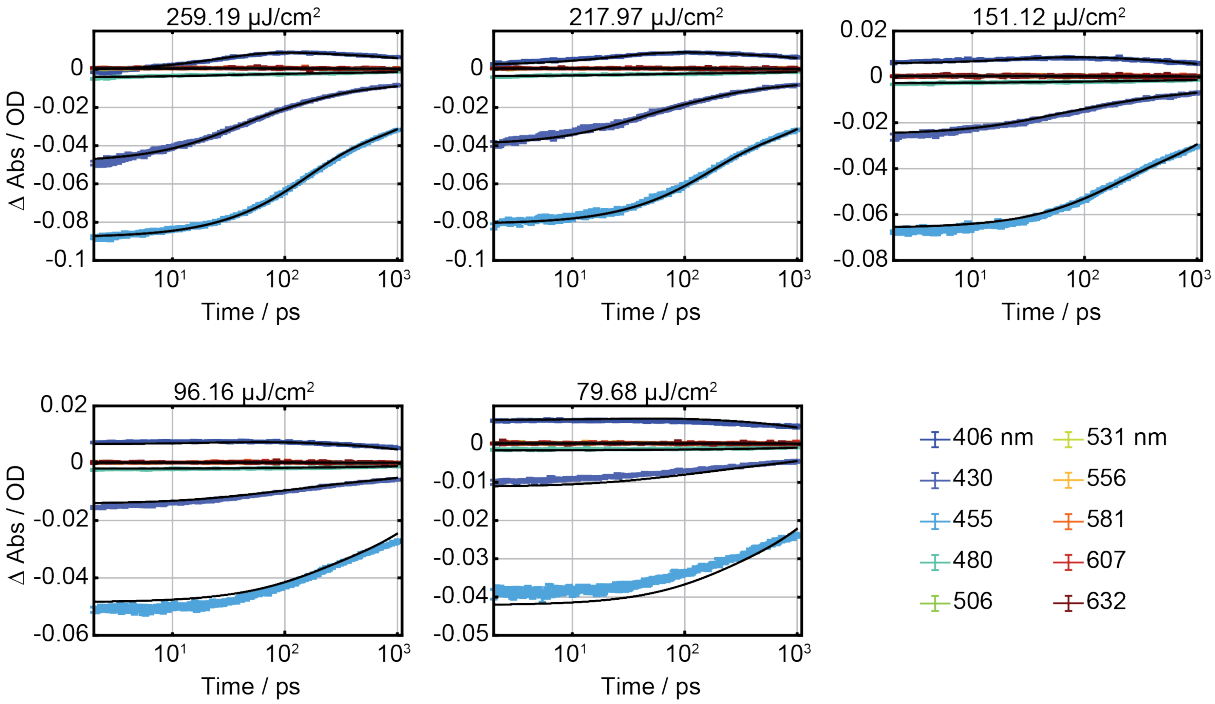

Figure S21. Kinetic traces and fits derived by Markov Chain Monte Carlo (MCMC) sampling of target model for non-illuminated TOPO-capped CdS nanorods. Each panel shows the experimental data and black lines represent the kinetic fit traces. The fit lines are plotted by drawing 100 random samples from the Markov Chain overlaid on top of each other with the same colour and linewidth to visually show the deviations among randomly drawn samples.

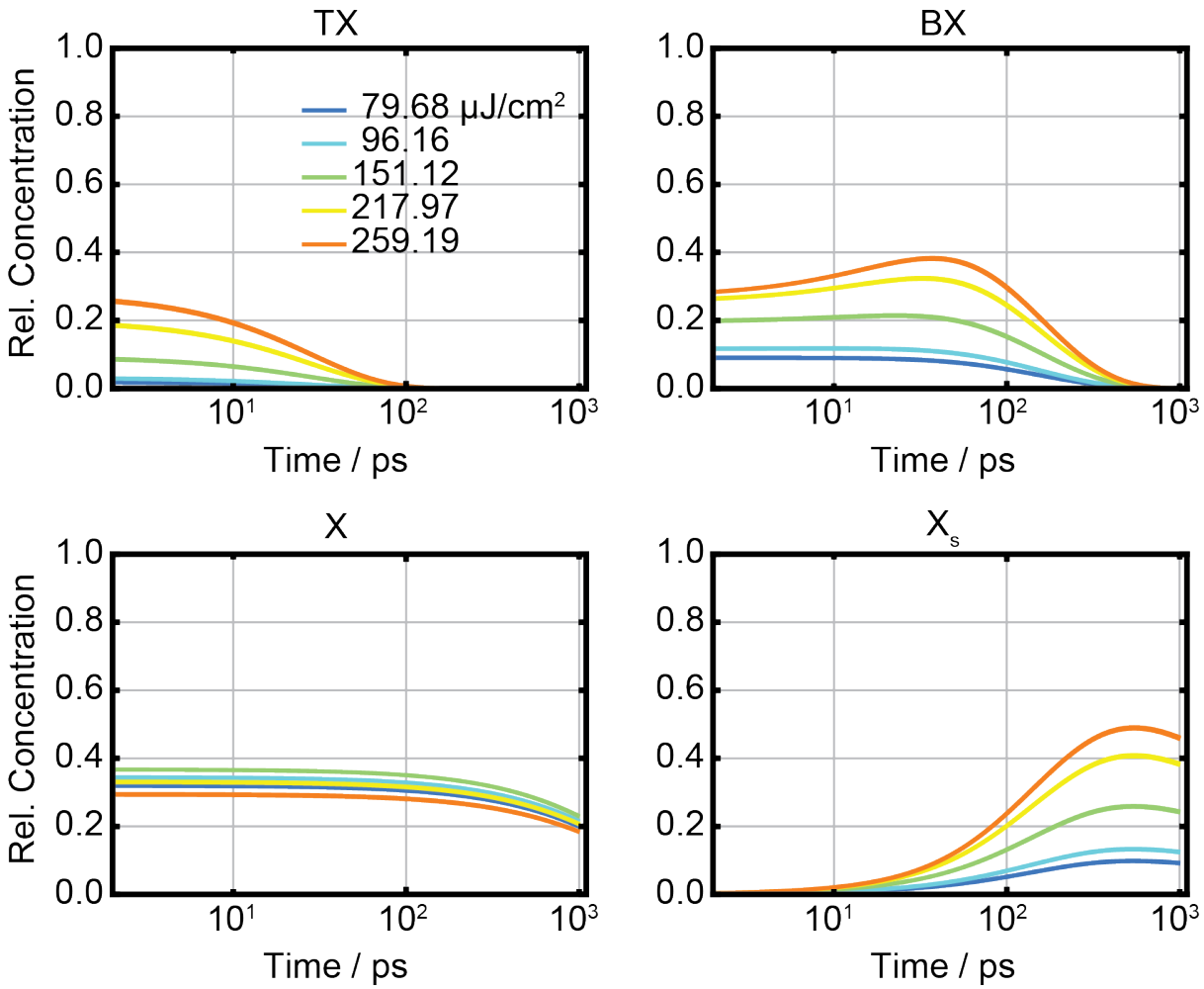

Figure S22. Intensity-dependent concentration profiles for non-illuminated TOPO-capped CdS nanorods were used for direct comparison with the CdS pre-illuminated sample. Excitonic species are given at the top of each panel. The concentration profiles are overlaid from 100 random samples drawn from the Markov Chain.

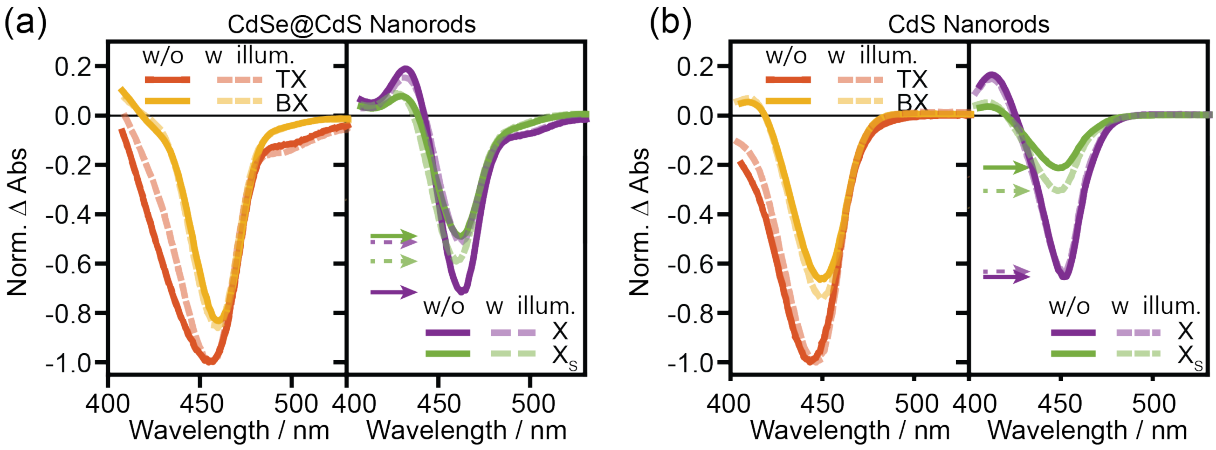

Figure S23. Influence of illumination on the modelled species associated spectra of nanorods excited with 400 nm pump pulse. Comparison of non-illuminated and illuminated SAS for CdSe@CdS (a) and CdS nanorods (b), normalized to their respective maximum tri-exciton bleach. The left panels in a&b show the comparison for higher order excitons, and the right panel shows the same for the two mono-excitons X and X_S. The dark solid curve represents the non-illuminated sample, and the light dashed curve represents the same species modelled after illuminated data. The wavelength region above 530 nm has been removed for clarity, and the same-style arrows represent the respective maximum bleach intensity.

Kinetic Modeling – testing various fitting models

Attempts to fit the experimental data with the Auger recombination model, including multiexcitonic species of the order five or even six were not successful. The results obtained using the MCMC fit is shown below (Figure S24–25). Though determining the quality of fit based on the error of fitted data is challenging due to very similar order of magnitude of errors, these models do not adequately describe the experimental data. The first point is that the lifetimes of higher-order exciton species for both models are random (see **Figure S24–S25**, lifetime values are shown in

Table S5) and do not follow a consistent decrease with exciton order, as expected for the Auger recombination process in nanorods.[1-4] Furthermore, in line with the non-systematic change in lifetime of the multiexciton species, the modelled spectral shapes do not follow the steady increase

in band-edge bleach signal of the CdS domain, as observed in the experimental data (Figure 1, main text). Due to these short comings of the results, it was concluded, that the cascade model is not suited to describe the data.

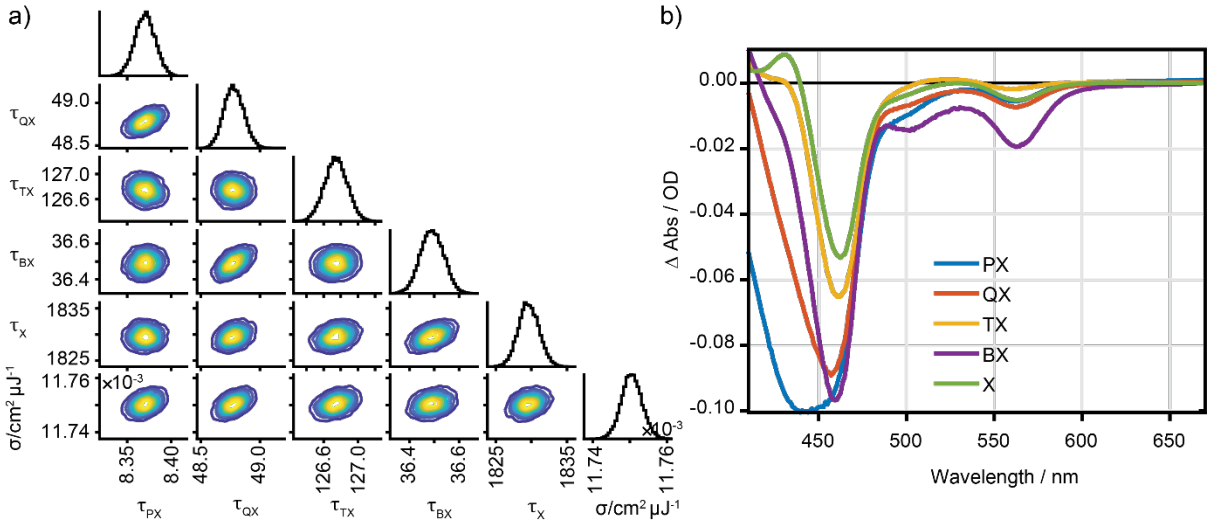

Figure S24. MCMC sampling using the cascade Auger recombination model using multiexciton species up to the 5th order. a) Corner plot of the posterior probability distribution for the modelled parameters. b) Calculated component spectra drawn from 100 random samples from the Markov Chain.

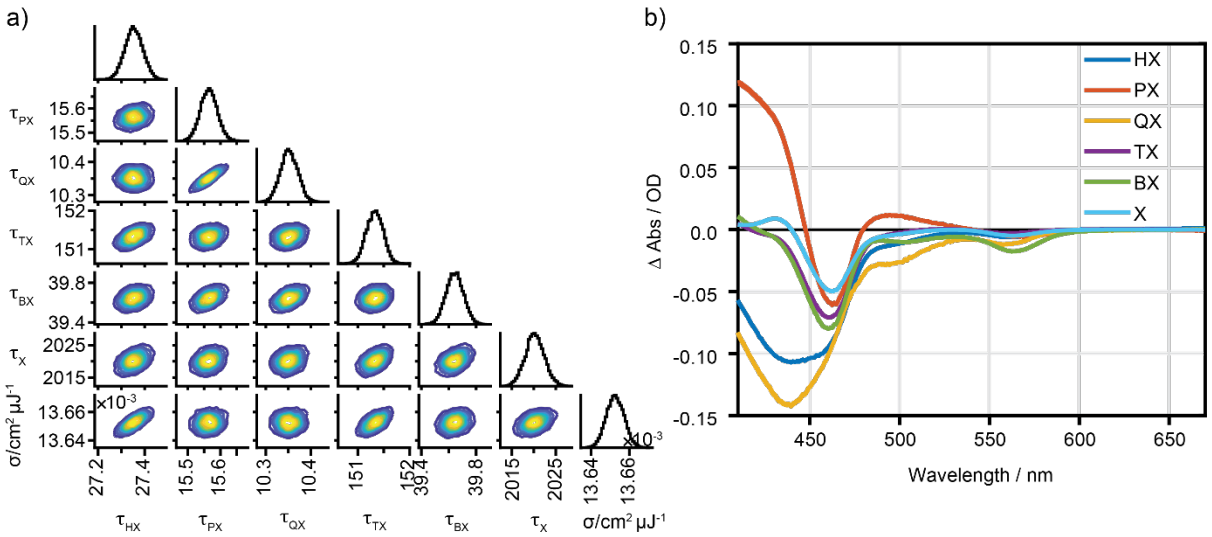

Figure S25. MCMC sampling using the cascade Auger recombination model using multiexciton species up to the 6th order. a) Corner plot of the posterior probability distribution for the modelled parameters. b) Calculated component spectra drawn from 100 random samples from the Markov Chain.

Table S5. Fitted median values and 95% confidence interval of five-exciton and six-exciton model parameters extracted from MCMC Sampling for TOPO-capped CdSe@CdS.

Parameter Name	Five exciton model	Six exciton model
$\tau_{hexaexciton}/ps$	--	$27.35^{27.43}_{27.28}$
$\tau_{pentaexciton}/ps$	$8.37^{8.39}_{8.35}$	$15.56^{15.62}_{15.51}$
$\tau_{tetraexciton}/ps$	$48.78^{48.95}_{48.62}$	$10.35^{10.39}_{10.32}$
$\tau_{triexciton}/ps$	$126.74^{127.00}_{126.48}$	$151.33^{151.63}_{151.01}$
$\tau_{biexciton}/ps$	$36.49^{36.58}_{36.40}$	$39.64^{39.77}_{39.52}$
$\tau_{monoexciton}/ps$[a]	1830^{1833}_{1827}	2020^{2025}_{2016}
Absorption cross-section $(\sigma)/\mathrm{cm^2\mu J^{-1}}$	$11.75 \cdot 10^{-3}{}^{11.76\times10^{-3}}_{11.74\times10^{-3}}$	$13.65 \cdot 10^{-3}{}^{13.66\times10^{-3}}_{13.64\times10^{-3}}$

Modifications of the kinetic function in the MCMC fitting routine

To incorporate the kinetic model described in the main text, we modified the following parts of the kinetic function of the previously published script.[7]

```
  K=[-params(1),0,0,0,0;
     params(1),-params(2),0,0,0;
     0,params(2),-params(3),0,0;
     0,0,0,-params(4),0;
     0,0,params(3),0,-params(5)];
```

and

```
  for i=1:numtrace
        %QX, TX, BX, X and XS source terms from Poisson distribution
        QXyield=1-poisscdf(3,params(end)*powers(i));
        TXyield=poisspdf(3,params(end)*powers(i));
        BXyield=poisspdf(2,params(end)*powers(i));
        Xyield=poisspdf(1,params(end)*powers(i));

        %Generate source term in component basis, generate matrix transform
        %that transforms source term to eigenbasis, evaluates dynamics, and
        %transforms back to the component basis
        source=[QXyield;TXyield;BXyield;Xyield;0];
        A2=Us*diag(Us\source);
        dyn(:,:,i)=A2*eigdyn;  %Dynamics evaluated at input time points
end
```

References

1. H. Zhu, Y. Yang and T. Lian, *Accounts. Chem. Res.*, 2013, **46**, 1270-1279.
2. Y. Ben-Shahar, J. P. Philbin, F. Scotognella, L. Ganzer, G. Cerullo, E. Rabani and U. Banin, *Nano Lett.*, 2018, **18**, 5211-5216.
3. V. I. Klimov, J. A. McGuire, R. D. Schaller and V. I. Rupasov, *Phys. Rev. B*, 2008, **77**, 195324.
4. H. Htoon, J. A. Hollingsworth, R. Dickerson and V. I. Klimov, *Phys. Rev. Lett.*, 2003, **91**, 227401.